nature COMMUNICATIONS

ARTICLE

Received 23 Apr 2013 | Accepted 2 Aug 2013 | Published 30 Aug 2013

DOI: 10.1038/ncomms3391

# Microwave magnetoelectric effect via skyrmion resonance modes in a helimagnetic multiferroic

Y. Okamura[1], F. Kagawa[1], M. Mochizuki[1,2], M. Kubota[3,4], S. Seki[1,5], S. Ishiwata[1], M. Kawasaki[1,3], Y. Onose[6] & Y. Tokura[1,3]

Magnetic skyrmion, a topologically stable spin-swirling object, can host emergent electromagnetism, as exemplified by the topological Hall effect and electric-current-driven skyrmion motion. To achieve efficient manipulation of nano-sized functional spin textures, it is imperative to exploit the resonant motion of skyrmions, analogously to the role of the ferromagnetic resonance in spintronics. The magnetic resonance of skyrmions has recently been detected with oscillating magnetic fields at 1–2 GHz, launching a search for new skyrmion functionality operating at microwave frequencies. Here we show a microwave magnetoelectric effect in resonant skyrmion dynamics. Through microwave transmittance spectroscopy on the skyrmion-hosting multiferroic crystal $Cu_2OSeO_3$ combined with theoretical simulations, we reveal nonreciprocal directional dichroism (NDD) at the resonant mode, that is, oppositely propagating microwaves exhibit different absorption. The microscopic mechanism of the present NDD is not associated with the conventional Faraday effect but with the skyrmion magnetoelectric resonance instead, suggesting a conceptually new microwave functionality.

[1] Department of Applied Physics and Quantum Phase Electronics Center, University of Tokyo, Tokyo 113 8656, Japan. [2] Department of Physics and Mathematics, Aoyama Gakuin University, Kanagawa 229 8558, Japan. [3] RIKEN Center for Emergent Matter Science (CEMS), Wako 351 0198, Japan. [4] Power Electronics R&D Unit, ROHM Co., Ltd., Kyoto 615 8585, Japan. [5] PRESTO, Japan Science and Technology Agency, Bunkyo, Tokyo 113 8656, Japan. [6] Department of Basic Science, University of Tokyo, Tokyo 153 8902, Japan. Correspondence and requests for materials should be addressed to Y.O. (email: okamura@cmr.t.u-tokyo.ac.jp).

A magnetic skyrmion, a vortex-like spin-swirling object (see inset of Fig. 1a), is now attracting considerable academic interests because it produces novel transport properties associated with its topological nature, such as topological Hall effect. Furthermore, as the size of magnetic skyrmions is typically 10–100 nm, they are potentially useful for next-generation spintronic devices with high information density[1,2]. Its crystalline form, the Skyrmion crystal (SkX), was studied theoretically[3] and was subsequently identified experimentally under a d.c. magnetic field $\mathbf{H}_{dc}$ in B20-type metallic chiral-lattice magnets, such as MnSi, (Fe,Co)Si and FeGe, through the reciprocal-space and real-space observations[4–7]. In those systems, the coupling of conduction electrons to the skyrmions potentially allows their manipulation via electric currents[8–11]. Recently, SkX has been discovered also in the insulating chiral magnet $Cu_2OSeO_3$ (Fig. 1a)[12–15]. This material hosts, as a multiferroic, a spin-texture mediated ferroelectric polarization $\mathbf{P}$, pointing to a possibility for nominally joule-heating-free, electric-field control of skyrmions via the magnetoelectric (ME) coupling. In fact, a recent experiment has demonstrated that d.c. electric fields exert a torque on SkX and induce its tilting[16]. We extend the idea of eletromagnetic action of SkX in insulators into a dynamical regime and exploit a resonantly enhanced response of magnetism to electric fields (ME resonance)[17,18]. In this context, various resonant modes lying at microwave frequencies in the multiferroic $Cu_2OSeO_3$ (ref. 19), such as the counterclockwise (CCW) and clockwise (CW) rotational modes (Fig. 1b,c, respectively) and a breathing mode of skyrmion (Fig. 1d), would be promising candidates for the microwave ME resonance[19–22].

In this work, we demonstrate the resonantly enhanced ME effect of these skyrmion modes through the microwave transmittance spectroscopy. This ME resonant character is accompanied by a new functionality that the absorption of an electromagnetic microwave by skyrmion motions depends on the direction of the incidence, that is, nonreciprocal directional dichroism (NDD). Furthermore, we address this phenomenon theoretically and find that the experimental results are well reproduced. The selection rule for the nonreciprocal effect is totally different from that of Faraday effect, indicating that the present NDD based on the skyrmion resonance may find novel application in microwave region.

## Results

**NDD via ME coupling**. The ME resonance in multiferroics involves the concomitant oscillations of $\mathbf{P}$ and magnetization $\mathbf{M}$; therefore, their interference with the $\mathbf{E}$ and $\mathbf{H}$ fields of electromagnetic wave may occur either constructively or destructively, which depends on the propagating vector $\mathbf{k}^{\omega}$ of electromagnetic wave[17,18]. When $\mathbf{P}$ and $\mathbf{M}$ oscillate constructively (destructively), the system can absorb electromagnetic waves more (less) efficiently. Thus, the ME resonance in multiferroics can lead to the nonreciprocal transmittance/absorption for a linearly polarized light: a phenomenon often called NDD. To detect microwave NDD as a hallmark of ME resonance, we carried out a two-port transmission spectroscopy on the coplanar waveguide circuit on which $Cu_2OSeO_3$ was mounted (Fig. 2a; see also Methods). The microwave in the coplanar waveguide is basically a linearly polarized light and propagates as a TEM mode, that is, both the magnetic and electric field of the microwave are perpendicular to $\mathbf{k}^{\omega}$. However, it should be noted that the polarization plane and hence the direction of $\mathbf{H}_{\omega}$ depend on the position in space: as shown in Fig. 2b, the $\mathbf{H}_{\omega}$ just above the center of signal line is parallel to the plane of the coplanar waveguide, whereas the $\mathbf{H}_{\omega}$ between the signal line and the ground is perpendicular to the plane. Thus, our experimental setup, which is based on the Voigt configuration ($\mathbf{H}_{dc} \perp \mathbf{k}^{\omega}$), includes not only $\mathbf{H}_{\omega}$ perpendicular to $\mathbf{H}_{dc}$ but also $\mathbf{H}_{\omega}$ parallel to $\mathbf{H}_{dc}$ (Fig. 2b). It follows that the present configuration using the coplanar waveguide allows all the resonant skyrmion motions; namely, two rotational modes (under $\mathbf{H}_{\omega} \perp \mathbf{H}_{dc}$) and one breathing mode (under $\mathbf{H}_{\omega} \parallel \mathbf{H}_{dc}$)[19,20].

**Experimental setup and selection rule**. To investigate the selection rule for NDD, we focus on the relation between $\mathbf{k}^{\omega}$ and $\mathbf{P} \times \mathbf{M}$ (refs 17,18). The important point is that the relation between $\mathbf{k}^{\omega}$ and $\mathbf{P} \times \mathbf{M}$ is relevant, whereas the direction of the $\mathbf{H}_{\omega}$ or $\mathbf{E}_{\omega}$ is irrelevant for the selection rule. From the symmetry

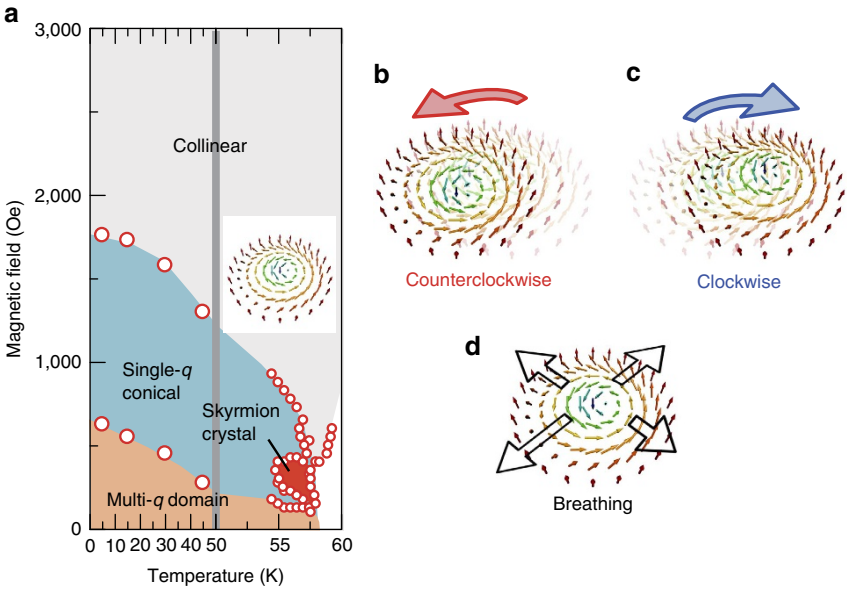


**Figure 1 | Spin excitations via microwave in the multiferroics $Cu_2OSeO_3$.** (**a**) Magnetic phase diagram under $\mathbf{H}_{dc} \parallel [110]$ determined by magnetic a.c. susceptibility measurement. The vertical line represents a change in scale. Inset illustrates the spin texture of a skyrmion. Each arrow represents the net magnetic moment. (**b**–**d**) Schematic illustration of skyrmion resonant motions: (**b**) CCW and (**c**) CW modes, where the core of skyrmion rotates in such a sense, and (**d**) a breathing mode, where the skyrmion oscillatingly shrinks and enlarges.

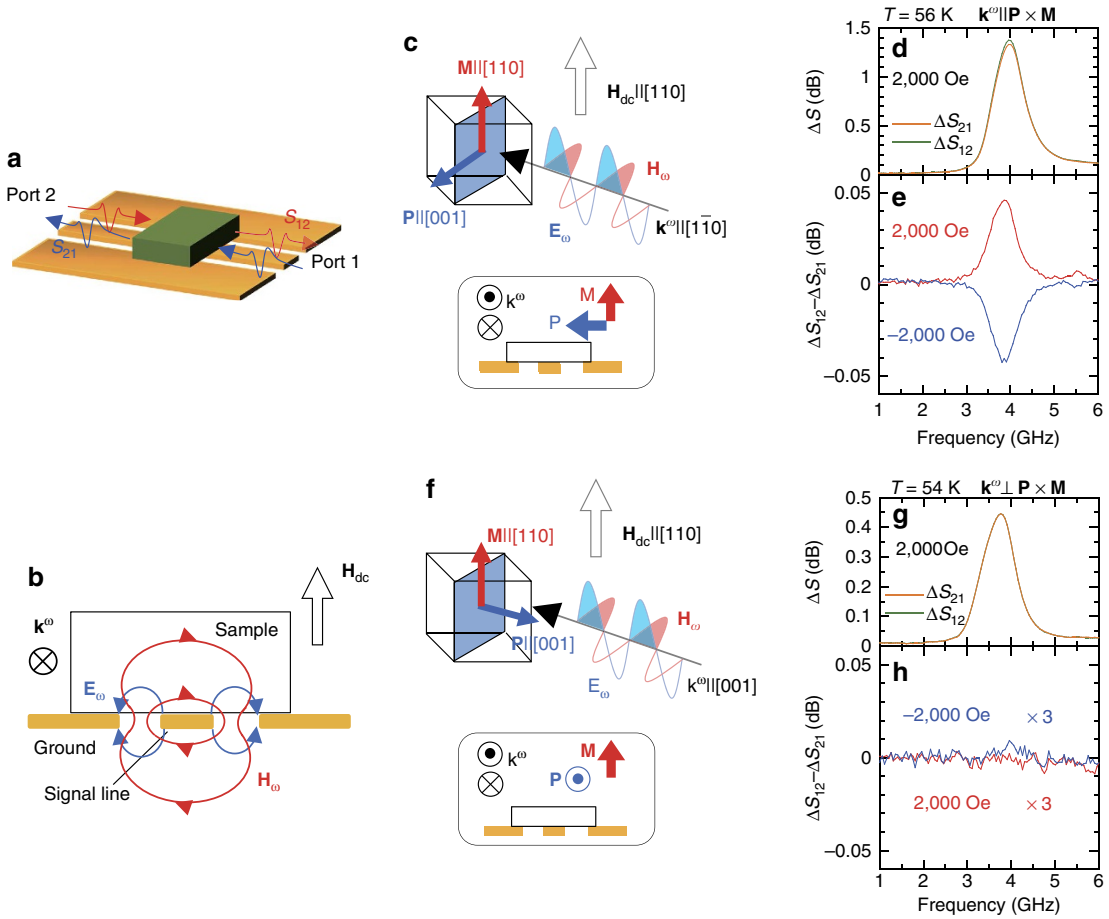


**Figure 2 | Selection rule for NDD.** (**a**) Schematic of the experimental setup. The sample size is roughly $1.5 \times 3.5 \times 0.5\,mm^3$. The microwave propagates along the coplanar waveguide in both directions. (**b**) Electromagnetic-field distribution in the present setup using a coplanar waveguide, viewed from the direction of microwave propagation. (**c**,**f**) Schematic illustrations for $\mathbf{k}^{\omega}\|\mathbf{P}\times\mathbf{M}$ configuration (**c**) and $\mathbf{k}^{\omega}\perp\mathbf{P}\times\mathbf{M}$ configuration (**f**). The magnetic field is applied along [110], which leads to $\mathbf{P}\|[001]$ and $\mathbf{M}\|[110]$ ($\|\mathbf{H}_{dc}$) (ref. 15). In the former configuration (**c**), $\mathbf{k}^{\omega}$ is set to along [1$\bar{1}$0], whereas in the latter configuration (**f**), $\mathbf{k}^{\omega}$ is set to along [001]. (**d**,**g**) Absorption spectra for microwave propagating from port 1 (2) to port 2 (1), $\Delta S_{21}$ ($\Delta S_{12}$) for the cases of $\mathbf{k}^{\omega}\|\mathbf{P}\times\mathbf{M}$ (**d**) and $\mathbf{k}^{\omega}\perp\mathbf{P}\times\mathbf{M}$ (**g**). (**e**,**h**) Nonreciprocal absorption spectra $\Delta S_{12}-\Delta S_{21}$ under positive and negative magnetic fields for the cases of $\mathbf{k}^{\omega}\|\mathbf{P}\times\mathbf{M}$ (**e**) and $\mathbf{k}^{\omega}\perp\mathbf{P}\times\mathbf{M}$ (**h**).

point of view, the NDD is emergent unless $\mathbf{P}\times\mathbf{M}$ is orthogonal to $\mathbf{k}^{\omega}$. However, there has been no report on the NDD associated with the ME resonance in a waveguide circuit, and we start with the verification of the selection rule in the field-induced collinear phase (Fig. 1a), where a ferrimagnetic resonance is expected via $\mathbf{H}_{\omega}\perp\mathbf{H}_{dc}$. To this end, we conducted the experiments under the two configurations: (i) $\mathbf{k}^{\omega}$ parallel to $\mathbf{P}\times\mathbf{M}$ (Fig. 2c) and (ii) $\mathbf{k}^{\omega}$ perpendicular to $\mathbf{P}\times\mathbf{M}$ (Fig. 2f). To achieve these configurations, $\mathbf{H}_{dc}$ along [110] was chosen, where $\mathbf{M}$ and $\mathbf{P}$ appear along [110] and [001], respectively, leading to $\mathbf{P}\times\mathbf{M}\|[1\bar{1}0]$ (ref. 15). Figure 2d,g presents the microwave absorption spectra measured under the ($\mathbf{k}^{\omega}\|\mathbf{P}\times\mathbf{M}$ ($\mathbf{k}^{\omega}\|[1\bar{1}0]$) and $\mathbf{k}^{\omega}\perp\mathbf{P}\times\mathbf{M}$ ($\mathbf{k}^{\omega}\|[001]$) configurations, respectively. The overall spectral shapes arising from the ferrimagnetic resonance are approximately similar to each other. Taking a closer look at Fig. 2d, however, one can find that the absorption of microwave propagating from port 2 to port 1 (denoted as $\Delta S_{12}$) is slightly larger than the case of the opposite propagation, $\Delta S_{21}$. For clarity, the $\Delta S_{12}-\Delta S_{21}$ spectrum under $\mathbf{H}_{dc}=+2{,}000$ Oe is plotted in Fig. 2e, where the nonreciprocal nature in the microwave absorption can be well discerned. To have a better understanding of the nonreciprocal absorption, we further investigated the $\Delta S_{12}-\Delta S_{21}$ spectrum under $\mathbf{H}_{dc}=-2{,}000$ Oe, because reversing $\mathbf{H}_{dc}$ ($\|\mathbf{M}$) should result in the sign reversal in $\mathbf{P}\times\mathbf{M}$ and hence in the $\Delta S_{12}-\Delta S_{21}$ spectrum[17,18]. In fact, we obtained the sign-inverted $\Delta S_{12}-\Delta S_{21}$ spectrum (Fig. 2e), in accord with the expectation.

Contrastingly, the $\Delta S_{12}-\Delta S_{21}$ spectrum under the configuration of $\mathbf{k}^{\omega}\perp\mathbf{P}\times\mathbf{M}$ turns out to exhibit no reciprocal nature with appreciable magnitude larger than the experimental accuracy (Fig. 2g,h), $\sim$0.09%, whereas the NDD magnitude is $\sim$3.3% in the $\mathbf{k}^{\omega}\|\mathbf{P}\times\mathbf{M}$ configuration (for the present definitions of the experimental accuracy and the NDD magnitude, see Methods). This observation is well accounted for by the expected selection rule for the NDD, namely, NDD disappears when $\mathbf{k}^{\omega}\perp\mathbf{P}\times\mathbf{M}$, ensuring that the nonreciprocal microwave absorption observed here is traced back not to experimental artifacts but to NDD inherent in $Cu_2OSeO_3$.

**ME resonance of skyrmions**. The nonreciprocal microwave absorption is expected also in the SkX phase because there exists finite $\mathbf{P}\times\mathbf{M}$. To see the microwave ME effect on the resonant skyrmion dynamics, we conducted the experiments with the $\mathbf{k}^{\omega}\|\mathbf{P}\times\mathbf{M}$ configuration and examined the magnetic-field dependence of the absorption spectra at 57 K. The results up to

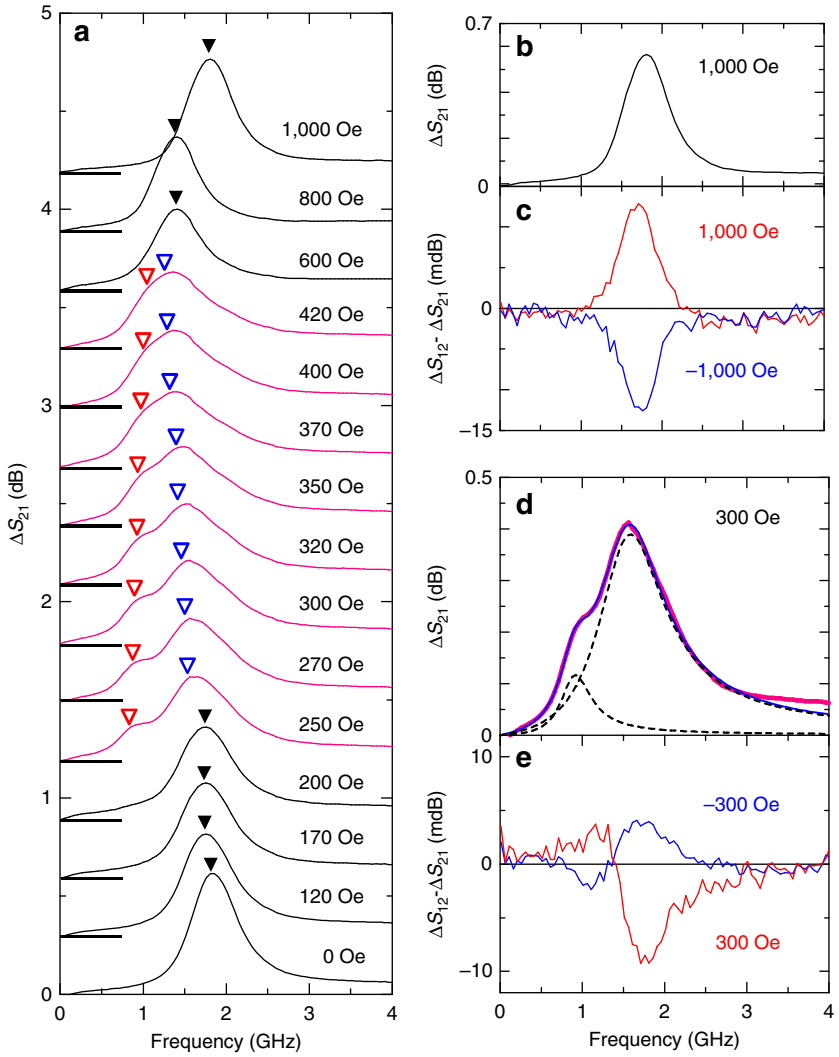


**Figure 3 | ME resonance spectra and NDD.** (**a**) Magnetic-field dependence of the absorption spectra at 57 K for the $\mathbf{k}^{\omega}\|\mathbf{P}\times\mathbf{M}$ configuration (that is, $\mathbf{P}\|[001]$, $\mathbf{M}\|\mathbf{H}_{dc}\|[110]$ and $\mathbf{k}^{\omega}\|[1\bar{1}0]$). Each spectrum is shifted upward for clarity; the offset levels are indicated by horizontal solid lines. The spectra in the SkX phase are highlighted by red colour. The triangles indicate the resonant frequencies. (**b**,**d**) Microwave absorption spectra at $\mathbf{H}_{dc}=1{,}000$ and 300 Oe, which corresponds to collinear and SkX, respectively. In (**d**), the results of two-peak fitting are also shown in addition to the raw data (red line): the broken lines represent each component, and the blue solid line is a sum of them. (**c**,**e**) Nonreciprocal absorption spectra at $\mathbf{H}_{dc}=\pm1{,}000$ Oe and $\pm300$ Oe.

$+1{,}000$ Oe are displayed in Fig. 3a. In the collinear phase ($\mathbf{H}_{dc}>700$ Oe) and conical phase ($\mathbf{H}_{dc}<250$ Oe and 420 Oe$<\mathbf{H}_{dc}<700$ Oe), each absorption spectrum in the present frequency window comprises a single peak due to the resonant mode in each magnetic state; correspondingly, the NDD spectrum with a single peak is observed (for example, Fig. 3c). In the intervening SkX phase at a intermediate field region, 250–420 Oe as determined by a.c. magnetic susceptibility (Fig. 4a), apparent two absorption bands are discerned around 1 GHz (open triangles in Fig. 3a). The overall spectra in this region can be reproduced by a superposition of two Lorentzians multiplied by frequency, and a typical fitting result is displayed in Fig. 3d (for more details, see Methods). Among these two absorptions, the lower-lying mode can be unambiguously assigned to the CCW rotational mode of skyrmion[19]. At the resonance frequency of the lower-lying CCW mode, the NDD spectra are clearly observed (Fig. 3e), demonstrating an ME resonant character of CCW rotational motion of skyrmion. In contrast, the origin of the higher-lying absorption in the SkX phase (Fig. 3d) has remained elusive, partly because the resonance frequency is quite close to that in the possible remnant domains of the conical phase. Furthermore, the CW rotational mode (Fig. 1c; allowed when $\mathbf{H}_{\omega}\perp\mathbf{H}_{dc}$) and the breathing mode (Fig. 1d; allowed when $\mathbf{H}_{\omega}\|\mathbf{H}_{dc}$) of skyrmion is anticipated to take place and be overlapped in this region, because the two modes have similar resonance frequencies[19,20] and our experimental setup produces a superposition of two linearly polarized lights, that is, $\mathbf{H}_{\omega}\perp\mathbf{H}_{dc}$ and $\mathbf{H}_{\omega}\|\mathbf{H}_{dc}$, as illustrated in Fig. 2b. Focusing on the NDD spectra under a positive magnetic field, however, we found that the higher-lying absorption in the SkX phase exhibits the negative NDD spectra (Fig. 3e), whereas only the positive NDD spectra are observed in other magnetic phases (Fig. 3c). This clearly indicates that the higher-lying absorption cannot share the same origin with that observed in the conical phase but should be attributed to the resonant skyrmion dynamics distinct from the CCW rotational motion.

**Comparison with the numerical calculation**. To identify the higher-lying resonant skyrmion dynamics with the ME character, we carried out a numerical calculation at zero temperature and examined the magnetic-field dependence of the resonance frequency, $\omega_R(\mathbf{H}_{dc})$, and the magnitude of NDD. Here we

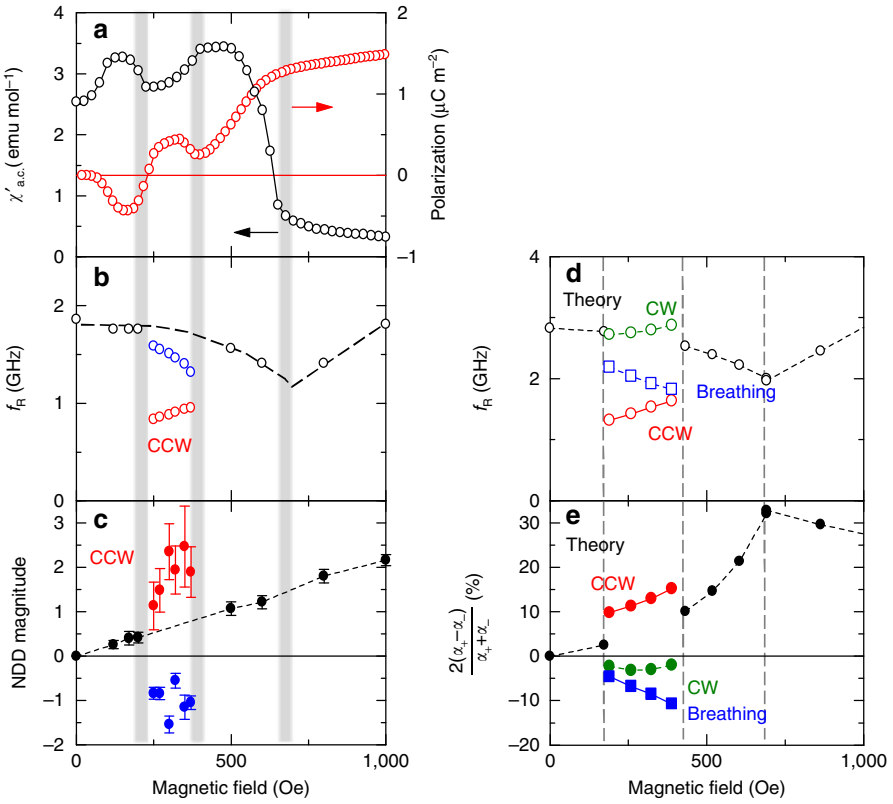


**Figure 4 | Comparison between experiment and theory of the skyrmion ME resonance.** (**a**–**c**) Magnetic-field dependence of a.c. magnetic susceptibility for $\mathbf{H}_{dc}\|[110]$ (**a**), the resonance frequency $\omega_R$ (**b**) and the normalized magnitude of nonreciprocal absorption for the $\mathbf{k}^{\omega}\|\mathbf{P}\times\mathbf{M}$ configuration (that is, $\mathbf{P}\|[001]$, $\mathbf{M}\|\mathbf{H}_{dc}\|[110]$ and $\mathbf{k}^{\omega}\|[1\bar{1}0]$). (**c**) In **a**, the electric polarization profile is also presented. Broken line in **b** is a guide to the eyes. (**d**,**e**) Theoretical simulation of the magnetic-field dependence of the resonance frequencies $\omega_R$ (**d**) and the magnitudes of the NDD normalized by the absorption coefficient (**e**). The thick vertical lines in **a**–**c** and the broken vertical lines in **d** and **e** represent the boundaries between different magnetic phases: from low to high fields, the magnetic phases are helical, SkX, conical and collinear. The error bars in Fig. 4c are associated with the variance of the nonreciprocal absorption in the off-resonant frequency range. For more details, see Methods. To check the reproducibility, the experiments were conducted four times, and the results were found to be reproducible.

employed a model Hamiltonian that is used in Mochizuki and Seki[22] (for details, see Methods) and known to reproduce the SkX under a magnetic field. The experimental results are plotted in Fig. 4b,c, whereas the numerical results are in Fig. 4d,e. Concerning the resonant modes in the helical, conical and collinear phases and the lower-lying CCW rotational mode in the SkX phase, we found that $\omega_R(\mathbf{H}_{dc})$ exhibits a good agreement between the experiment and theory; moreover, the magnetic-field evolutions of NDD are also consistent at least on a qualitative level (Fig. 4c,e). Regarding the higher-lying mode, the experimental $\omega_R(\mathbf{H}_{dc})$ (Fig. 4b) coincides with that of the breathing mode in the simulations rather than the CW rotational mode (Fig. 4d); therefore, the skyrmion motion at the higher-lying absorption is ascribed to the breathing mode. It is worth mentioning that not only the behaviour of $\omega_R(\mathbf{H}_{dc})$ but also the signs of NDD are consistent between the experiments and theory in all the magnetic phases. A large difference in magnitude of NDD between the experiments (Fig. 4c) and the zero-temperature simulations (Fig. 4e) can be reasonably attributed to a thermal contraction of magnetic moments at a measurement temperature ($\sim$57 K) close to the paramagnetic phase boundary.

## Discussion

As a whole, the magnitude of NDD increases with a magnetic field (Fig. 4c); this may be explained qualitatively by increase in the net magnetization **M** and electric polarization **P**. However, some observations should be interpreted beyond the phenomenological understanding of NDD based on $\mathbf{P}\times\mathbf{M}$. First, the NDD does not change its sign when **P** is reversed. The sign of **P** is negative in the lower-field conical phase ($\mathbf{H}_{dc}<250$ Oe) and positive in the higher-field conical phase (420 Oe$<\mathbf{H}_{dc}<$700 Oe), whereas the NDD is positive for the both phases (Fig. 4c). Second, although the magnitudes of **P** and **M** in the SkX phase is not so different from those in the conical phases, the NDD signal in the SkX phase shows an appreciable enhancement. Finally, the sign and magnitude in NDD are different between the different resonant skyrmion motions, for example, CCW rotational mode versus breathing mode. These observations clearly suggest that understanding of the entanglement between local electric and magnetic dipoles and their dynamics is crucial for the emergent microwave NDD.

In conclusion, we have conducted the microwave transmittance spectroscopy and numerical simulation on the multiferroic helimagnet $Cu_2OSeO_3$ to prove the ME character of the skyrmion resonant mode by observing microwave NDD. It has been confirmed that the selection rule, $\mathbf{k}^{\omega}\|\mathbf{P}\times\mathbf{M}$, holds for the microwave NDD effect as well; the NDD vanishes when $\mathbf{k}^{\omega}\perp\mathbf{P}\times\mathbf{M}$. The theoretical simulations have successfully reproduced the experimental observations regarding the sign and the magnetic-field dependence of NDD. This skyrmion ME effect will open a new avenue for the skyrmion-based microwave functionalities.

## Methods

**Sample preparation and characterization.** Single crystal of $Cu_2OSeO_3$ was prepared by chemical vapour transport[12]. Magnetic a.c. susceptibility was measured with a SQUID magnetometer (MPMS; Quantum Design).

**Microwave transmittance spectroscopy.** The broadband microwave transmission spectroscopy was carried out by using a vector network analyser (E8363C; Agilent Technology), with the sample mounting on a coplanar waveguide. The $\mathbf{H}_{dc}$ ($\|\mathbf{M}$) was applied along [110] throughout the experiments, in which configuration the finite $\mathbf{P}$ appears along [001], orthogonal to $\mathbf{H}_{dc}$ (ref. 15). We define the absorption spectrum due to magnetic excitation $\Delta S_{21(12)}(\omega, \mathbf{H}_{dc})$ as $\Delta S_{21(12)}(\omega, \mathbf{H}_{dc}) = S_{21(12)}(\omega, 5{,}000\,\mathrm{Oe}) - S_{21(12)}(\omega, \mathbf{H}_{dc})$, where $S_{21(12)}(\omega, \mathbf{H}_{dc})$ denotes a transmittance spectrum at $\mathbf{H}_{dc}$: the resonance frequency at 5,000 Oe is beyond 8 GHz and can therefore be regarded as the system background as far as our frequency window (0.01–6 GHz) is considered. To avoid the possible effect of hysteresis, we first applied $\mathbf{H}_{dc}$ up to 5,000 Oe and then decreased $\mathbf{H}_{dc}$ to the target field. The definition of the resonance frequency $\omega_R$ and the NDD magnitude are as follows: at a given magnetic field in the conical or ferrimagnetic phases (for example, Fig. 3b), we define $\omega_R$ as the peak frequency in the absorption spectra and the magnitude of NDD as $2(\Delta S_{12}(\omega_R) - \Delta S_{21}(\omega_R))/(\Delta S_{12}(\omega_R) + \Delta S_{21}(\omega_R))$. In the SkX phase (for example, Fig. 3d), we found that the overall absorption spectra can be well reproduced by a superposition of two Lorentzians multiplied by frequency, that is, $\left(A\omega/\left((\omega-\omega_{R1})^2+B\right)\right)+\left(C\omega/\left((\omega-\omega_{R2})^2+D\right)\right)$, where $A$, $B$, $C$, $D$, $\omega_{R1}$ and $\omega_{R2}$ are all fitting parameters, as shown in Fig. 3d. The errors in estimating each NDD magnitude were defined as the variance of $\Delta S_{12} - \Delta S_{21}$ in the off-resonant regime divided by the peak value of each component.

**Numerical calculation of the dynamical ME tensor.** We employed a two-dimensional classical Heisenberg model that contains the ferromagnetic-exchange interaction, the Dzyaloshinskii–Moriya interacion and the Zeeman coupling to $\mathbf{H}_{dc}$. The parameters in the Hamiltonian were chosen so as to reproduce experimental values of the helical period and the critical magnetic fields that separate the different magnetic phases[12]. A local polarization at each site was evaluated within the *d*–*p* hybridization model[15,23,24], and we calculated the temporal evolution of spins and polarizations after applying a microwave pulse by solving the Landau–Lifshitz–Gilbert equation numerically. Then, we obtained their Fourier tranforms and derived the ME tensors. For more details, see Mochizuki and Seki[22].

## References


1. Fert, A., Cros, V. & Sampaio, J. Skyrmions on the track. *Nat. Nanotech.* **8,** 152–156 (2013).
2. Rosch, A. Skyrmions: moving with the current. *Nat. Nanotech.* **8,** 160–161 (2013).
3. Rößler, U. K., Bogdanov, A. N. & Pfleiderer, C. Spontaneous skyrmion ground states in magnetic metals. *Nature* **442,** 797–801 (2006).
4. Mühlbauer, S. *et al.* Skyrmion lattice in a chiral magnet. *Science* **323,** 915–919 (2009).
5. Münzer, W. *et al.* Skyrmion lattice in the doped semiconductor $Fe_{1-x}Co_xSi$. *Phys. Rev. B* **81,** 041203 (2010).
6. Yu, X. Z. *et al.* Real-space observation of a two-dimensional Skyrmion crystal. *Nature* **465,** 901–904 (2010).
7. Yu, X. Z. *et al.* Near room temperature formation of a Skyrmion crystal thin-films of the helimagnet FeGe. *Nat. Mat.* **10,** 106–109 (2011).
8. Neubauer, A. *et al.* Topological hall effect in the *A* phase of MnSi. *Phys. Rev. Lett.* **102,** 186602 (2009).
9. Jonietz, F. *et al.* Spin transfer torques in MnSi at ultra-low current densities. *Science* **330,** 1648–1651 (2010).
10. Yu, X. Z. *et al.* Skyrmion flow near room temperature in an ultralow current density. *Nat. Comm.* **3,** 988 (2012).
11. Schultz, T. *et al.* Emergent electrodynamics of Skyrmions in a chiral magnet. *Nat. Phys.* **8,** 301–304 (2012).
12. Seki, S., Yu, X. Z., Ishiwata, S. & Tokura, Y. Observation of Skyrmions in a multiferroic material. *Science* **336,** 198–201 (2012).
13. Adams, T. *et al.* Long-wavelengh helimagnetic order and Skyrmion lattice phase in $Cu_2OSeO_3$. *Phys. Rev. Lett.* **108,** 237204 (2012).
14. Bos, J.-W. G., Colin, C. V. & Palstra, T. T. M. Magnetoelectric coupling in the cubic ferrimagnet $Cu_2OSeO_3$. *Phys. Rev. B* **78,** 094416 (2008).
15. Seki, S., Ishiwata, S. & Tokura, Y. Magnetoelectric nature of Skyrmion in a chiral magnetic insulator $Cu_2OSeO_3$. *Phys. Rev. B* **86,** 06403 (2012).
16. White, J. S. *et al.* Electric field control of the skyrmion lattice in $Cu_2OSeO_3$. *J. Phys. Condens. Matter* **24,** 432201 (2012).
17. Takahashi, Y. *et al.* Magnetoelectric resonance with electromagnons in a perovskite helimagnet. *Nat. Phys.* **8,** 121–125 (2011).
18. Kézsmárki, I. *et al.* Enhanced directional dichroism of terahertz light in resonance with magnetic excitation of the multiferroic $Ba_2CoGe_2O_7$ oxide compound. *Phys. Rev. Lett.* **106,** 057403 (2011).
19. Onose, Y., Okamura, Y., Seki, S., Ishiwata, S. & Tokura, Y. Observation of magnetic excitations of Skyrmion crystal in a helimagnetic insulator $Cu_2OSeO_3$. *Phys. Rev. Lett.* **109,** 037603 (2012).
20. Mochizuki, M. Spin-wave and their intense excitation effects in Skyrmion crystals. *Phys. Rev. Lett.* **108,** 017601 (2012).
21. Petrova, O. & Tchernyshyov, O. Spin waves in a skyrmion crystal. *Phys. Rev. B* **84,** 214433 (2011).
22. Mochizuki, M. & Seki, S. Magnetoelectric resonances and predicted microwave diode effect of skyrmion crystal in multiferroic chiral-lattice magnet. *Phys. Rev. B* **87,** 134403 (2013).
23. Jia, C., Onoda, S., Nagaosa, N. & Han, J.-H. Microscopic theory of spin-polarization coupling in multiferroic transition metal oxides. *Phys. Rev. B* **76,** 144424 (2007).
24. Arima, T. Ferroelectricity induced by proper-screw type magnetic order. *J. Phys. Soc. Jpn* **76,** 073702 (2007).


## Acknowledgements

We thank Y. Takahashi, S. Bordács and K. Shibata for fruitful discussions and K. Kanoda for experimental supports. This work was supported by the Grant-in-Aid for Scientific Research (Grant Nos 24224009, 24684020, 24226002, 25870169, 25287088 and 25247058) from the JSPS, Murata Science foundation and Funding Program in World-Leading Innovative R&D on Science and Technology (FIRST Program).

## Author contributions

Y.Ok., F.K. and Y.On. carried out the microwave transmission measurement and measured the magnetic a.c. susceptibility. Y.Ok., M.Ku. and M.Ka. made a coplanar waveguide. S.S. and S.I. prepared the sample. M.M. conducted numerical calculations. F.K. and Y.T. conceived the project. Y.Ok., F.K. and Y.T. jointly analysed and interpreted the results and wrote the manuscript.

## Additional information

**Competing financial interests:** The authors declare no competing financial interests.

**Reprints and permission** information is available online at http://npg.nature.com/reprintsandpermissions/

**How to cite this article:** Okamura, Y. *et al.* Microwave magnetoelectric effect via skyrmion resonance modes in a helimagnetic multiferroic. *Nat. Commun.* 4:2391 doi: 10.1038/ncomms3391 (2013).